

Published in final edited form as:

Nature. 2010 January 21; 463(7279): 360–363. doi:10.1038/nature08672.

Systematic sequencing of renal carcinoma reveals inactivation of histone modifying genes

Gillian L. Dalgliesh¹, Kyle Furge², Chris Greenman¹, Lina Chen¹, Graham Bignell¹, Adam Butler¹, Helen Davies¹, Sarah Edkins¹, Claire Hardy¹, Calli Latimer¹, Jon Teague¹, Jenny Andrews¹, Syd Barthorpe¹, Dave Beare¹, Gemma Buck¹, Peter J. Campbell¹, Simon Forbes¹, Mingming Jia¹, David Jones¹, Henry Knott¹, Chai Yin Kok¹, King Wai Lau¹, Catherine Leroy¹, Meng-Lay Lin¹, David J McBride¹, Mark Maddison¹, Simon Maguire¹, Kirsten McLay¹, Andrew Menzies¹, Tatiana Mironenko¹, Lee Mulderrig¹, Laura Mudie¹, Sarah O'Meara¹, Erin Pleasance¹, Arjunan Rajasingham¹, Rebecca Shepherd¹, Raffaella Smith¹, Lucy Stebbings¹, Philip Stephens¹, Gurpreet Tang¹, Patrick S Tarpey¹, Kelly Turrell¹, Karl J. Dykema², Sok Kean Khoo³, David Petillo³, Bill Wondergem², John Anema⁴, Richard J. Kahnoski⁴, Bin Tean Teh^{3,5}, Michael R. Stratton^{1,6}, and P. Andrew Futreal¹

¹Cancer Genome Project, Wellcome Trust Sanger Institute, Hinxton, CB10 1SA UK

²Laboratory of Computational Biology, Van Andel Research Institute, Grand Rapids, MI 49503 USA

³Laboratory of Cancer Genetics, Van Andel Research Institute, Grand Rapids, MI 49503 USA

⁴Department of Urology, Spectrum Health Hospital, Grand Rapids, MI 49503, USA

⁵NCCS-VARI Translational Cancer Research Laboratory, National Cancer Centre, 169610 Singapore

⁶Institute of Cancer Research, Sutton, Surrey SM2 5NG, UK

Abstract

Clear cell renal cell carcinoma (ccRCC) is the most common form of adult kidney cancer, characterised by the presence of inactivating mutations in the *VHL* gene in the majority of cases^{1,2} and by infrequent somatic mutations in known cancer genes. To elucidate further the genetics of ccRCC, we have sequenced 101 cases through 3544 protein coding genes. Here we report the identification of inactivating mutations in two genes encoding enzymes involved in histone modification, *SETD2*, a histone H3 lysine 36 methyltransferase and *JARID1C (KDM5C)*, a histone H3 lysine 4 demethylase in addition to mutations in the histone H3 lysine 27 demethylase, *UTX (KMD6A)*, we recently reported³. The results highlight the role of mutations in components of the chromatin modification machinery in human cancer. Additionally, *NF2* mutations were found in non-VHL mutated ccRCC and several other likely cancer genes were identified. These results indicate that substantial genetic heterogeneity exists in a cancer type dominated by mutations in a single gene and that systematic screens will be key to fully elucidating the somatic genetic architecture of cancer.

Correspondence should be addressed to BTT (Bin.Teh@vai.org), MRS (mrs@sanger.ac.uk) and PAF (paf@sanger.ac.uk).

Author Contributions:

GLD directed the analytical aspects of the study. KF, KJD and LC performed the expression analyses. CG contributed statistical analyses. GB, HD, SE, CH, JT, AB,JA,SB, DB, GB, PJC, SF, MJ, DJ, HK, CYK, CL, ML, DJM, MM, SM, KM, AM, TM, LM, LM, SO, EP, AR, RS, RS, LS, PS, GT, PST, KT performed the sequencing, copy number, data analyses and provided comments on the manuscript. JA, RJK, SKK, DP, BW and BTT contributed samples, data and comments on the manuscript. MRS and PAF conceived and directed the study and wrote the manuscript.

Renal cell carcinoma accounts for about 209,000 new cases per year worldwide and 102,000 deaths². Compared to other adult carcinomas, the genetics of ccRCC are distinctive. The majority of ccRCC have either somatic or germline inactivating mutations in the *VHL* gene, which are absent in most other cancers. Known cancer genes that are frequently mutated in other adult epithelial cancers, for example the *RAS* genes, *BRAF*, *TP53*, *RB*, *CDKN2A*, *PIK3CA*, *PTEN*, *EGFR* and *ERBB2*, make only a small contribution to ccRCC (<http://www.sanger.ac.uk/genetics/CGP/cosmic/>). To further elucidate the somatic genetics of ccRCC, we sequenced the coding exons of 3544 genes using sequencing in 101 ccRCC (Supplementary Table 1 for sample information) equating to approximately 745 Mb of cancer genome sequenced. A full list of genes is given in Supplementary Table 2 and available online (<http://www.sanger.ac.uk/genetics/CGP/Studies/>). Copy number analyses using high-density SNP array and genome-wide expression array analyses were also performed. The initial study was comprised of 96 primary pre-treatment tumours (Table 1) and 5 ccRCC cell lines for which there was a matching lymphoblastoid line. All somatic mutations were confirmed by sequencing of the relevant exons in normal DNAs from the same individuals.

515 somatic base substitutions and small insertions/deletions were identified in the initial study (Supplementary Table 3). This included 56 cases (55%) with mutations in *VHL*, a prevalence in agreement with other reports⁴. Evaluation of gene expression revealed two distinct phenotypes (Figure 1a). Seventy five out of 91 (82%) ccRCCs assessed for expression had up-regulation of genes associated with cellular hypoxia^{5,6} with most (49/75, 65%) carrying *VHL* inactivating point mutations. Loss of 3p where *VHL* resides was the most frequent (88/101, 87%) copy number change seen on SNP array analyses. (Supplementary Figure 2; <http://www.sanger.ac.uk/cgi-bin/genetics/CGP/cghviewer/CghHome.cgi>). We identified a significantly ($p < 0.001$, Supplemental Methods) higher proportion of small insertion/deletion mutations in ccRCC than seen in screens of the coding exons in pancreatic cancer⁷ and glioma⁸ or several cancer types screened through all protein kinase genes⁹. This may indicate an unidentified DNA repair defect, a common exposure or combination of these two. Average mutation prevalence was 0.75/Mb, somewhat lower than that observed for other adult cancers⁹. The mutation spectrum in ccRCC was unremarkable, being dominated by C to T/G to A transitions (Supplementary Figure 1) as has been noted in several other adult cancers⁹.

Genes with two or more non-synonymous mutations, a subset of those with at least one truncating mutation and/or identified as being of particular interest (Supplementary Table 5) were sequenced in a follow-up series of 311 primary RCC samples comprised of 246 ccRCC plus 65 additional samples of non-clear cell histology. Combined initial and follow-up screening data (Supplementary Tables 3 and 6) minus *VHL* mutations, were subjected to statistical analyses for the presence of positive selection, i.e. clustering of somatic mutations in a subset of genes consistent with a role in cancer development (Supplementary Methods). Five genes (*SETD2*, *JARID1C*, *NF2*, *UTX*, *MLL2*) have statistical support for being under selection at $FDR < 0.2$, with all but *MLL2* having strongest evidence for selection by truncating mutations (Supplementary Table 7).

Twelve of 407 (3%) ccRCC cases had somatic truncating mutations in *SETD2*, which encodes a histone H3K36 methyltransferase¹⁰, and 13/407 (3%) had truncating mutations in *JARID1C*, which encodes a histone H3K4 demethylase¹¹ (Table 2, Supplementary Table 8). Screening of 779 cancer cell lines identified an additional *SETD2* homozygous truncating mutation in the A498 ccRCC line. As assessment of homozygous deletions in primary tumour material is challenging, it is possible that we have underestimated the prevalence of inactivating mutations in these genes. No mutations were found in either *SETD2* or *JARID1C* in the subset of non-clear cell cancers included in the follow-up screen

and there was little evidence for involvement in other tumour types in cancer cell lines (Supplementary Table 9) in contrast to UTX. 88% (21/24) of samples with truncating *SETD2* and *JARID1C* mutations had *VHL* mutations and/or the hypoxia expression phenotype (Figure 1a, b). One ccRCC cell line, LB996-RCC, was found to harbour (in addition to a *NF2* truncating mutation) both a truncating *UTX* and *SETD2* mutation, suggesting that these are not redundant in ccRCC development.

Comparison of expression phenotypes of *SETD2* and *JARID1C* mutated ccRCCs revealed a signature for both and marked difference between the two (Figure 2a, Supplementary Table 10a, b). Large scale transcriptional deregulation was noted in the *SETD2* mutated subset with 298 genes showing significant differences (FDR<0.05, P=0.001 for association with *SETD2* mutation) in expression relative to other cancers analysed (Figure 2b, Supplementary Table 10a). Nearly all of the significant expression changes were two-fold or less. In contrast, *JARID1C* mutant cancers revealed a much more restricted signature (Figure 2c, Supplementary Table 10b). Eighteen genes had significant changes in expression (FDR<0.05) in cancers with *JARID1C* mutations, including the metallothionein genes. Of note, those ccRCC with *UTX* mutations were also found to over-express metallothioneins (Figure 2c,d, Supplementary Table 10c) suggesting overlap in transcriptional deregulation caused by *JARID1C* and *UTX* loss (Figure 2e). Indeed, *UTX* and *JARID1C* are both implicated in H3K4 methylation status, *JARID1C* directly as a H3K4 demethylase¹¹ and *UTX* as a component of the MLL2/3 H3K4 methylation complex^{12, 13}. In support of the importance of this axis, *MLL2*, an H3K4 methylase, was one of the other genes identified as a likely ccRCC cancer gene in our statistical analyses.

Five somatic truncating mutations in the *NF2* gene were found in the full screen (Table 2, Supplementary Table 8). Germline *NF2* truncating mutations predispose to neurofibromatosis II, characterised by predisposition to acoustic neuromas, meningiomas and schwannomas¹⁴. Somatic truncating mutations have been reported in these tumour types as well as mesothelioma (<http://www.sanger.ac.uk/genetics/CGP/cosmic/>). Sequencing in 779 cancer cell lines identified two truncating mutations in ccRCC cell lines SN12C and ACHN (<http://www.sanger.ac.uk/genetics/CGP/CellLines/>), supporting a novel role for *NF2* in ccRCC. In contrast to *JARID1C* and *SETD2*, none of the *NF2* mutant ccRCC samples harboured a *VHL* mutation or exhibited the hypoxia expression phenotype (Figure 1a, b). These data suggest that somatic *NF2* mutations may account for a proportion of this subset of cases.

The screen identified a number of other potential new cancer genes in ccRCC (Table 2, Supplementary Table 8), including the identification of three samples with somatic *HIF1a* truncating mutations. Only these truncating mutations were found and two of the three samples had *VHL* point mutations. It has been shown that HIF1a and HIF2a have overlapping but non-identical targets and activities. HIF1a antagonises MYC function whilst HIF2a cooperates with MYC^{15,16}. In *VHL* disease-associated ccRCC frequent absence of HIF1a staining with a preponderance of HIF2a positivity has been reported¹⁷, suggesting that there may be selection for loss of HIF1a during ccRCC progression. Three different truncating mutations (Table 2, Supplementary Table 8) were also identified in the DNA mismatch repair gene, *PMS1*. Notably, two truncating mutations found in the follow-up screen proved to be germline alleles. To our knowledge this is the first report of *PMS1* mutations in ccRCC. Both germline cases were late onset (70 and 71 years old), without documented family history and none of the three mutated cancers were microsatellite unstable (data not shown). No truncating variants were detected in sequencing all coding exons of *PMS1* in 528 normal controls indicating the germline alleles are not polymorphisms. Determining the extent truncating germline *PMS1* alleles contribute to ccRCC will require larger cohort studies.

Somatic truncating mutations were detected in both initial and follow-up screens in *WRN*, *NBN* and *ZUBR1(UBR4)* (Table 2, Supplementary Table 8). *WRN* and *NBN* are both involved in DNA double strand break repair¹⁸ and recessive mutations in *WRN* and *NBN* give rise to Werner syndrome and Nijmegen breakage syndrome, respectively, both which predispose to cancer^{19,20} *ZUBR1* encodes the p600 retinoblastoma associated protein and has been shown to be a cellular target for the bovine papilloma virus 21 and human papilloma type 16 E7 proteins²². Interaction of E7 with p600 has been shown to mediate cellular transformation independent of RB1 binding^{21,22} and knockdown of p600 in the absence of E7 induces anchorage independent growth²².

VHL inactivation alone induces senescence, suggesting a requirement for additional mutations to further drive ccRCC development in *VHL* mutant cases²³. Conditional knockout of the *VHL* gene in renal epithelium does not generate any RCC phenotype, consistent with a need for additional hits (Teh, unpublished results). The mutations in the genes reported here likely contribute in this regard and the work further suggests that there are likely to be other mutated genes in ccRCC. As exemplified here, even in the context of a very prevalent driver mutation and dominant histological subtype, the numbers of cancers needed to adequately explore and capture the somatic genetic heterogeneity may be quite large, strongly supporting current efforts to expand mutational screening to large sample series with ultimately full genome sequencing of hundreds of cancers of all major subtypes (<http://www.icgc.org/>). For ccRCC, the data presented here will provide insights into its pathogenesis and the opportunity to understand the role of genetic subtypes in clinical behaviour and response to treatment.

Methods Summary

Genomic DNA samples were obtained from clinical tumour samples (>80% tumour cellularity), matching peripheral blood/adjacent normal kidney taken at nephrectomy and cancer cell lines as indicated utilizing standard protocols. Collection and use of patient samples were approved by the appropriate IRB of each Institution in addition to this study having LREC approval locally. RCC clinical samples and cell lines screened are given in Supplemental Table 1. SNPArray hybridization on the SNP6.0 platform was as per Affymetrix Protocols and as as described at <http://www.sanger.ac.uk/cgi-bin/genetics/CGP/cghviewer/CghHome.cgi>. PCR-based exon resequencing was performed and data analysed as previously described⁹ with sequencing traces being first analysed using a semiautomated system²⁴ followed by manual inspection. PCR primer sequences are available for download at <http://www.sanger.ac.uk/genetics/CGP/Studies/Renal/>. Overall significance of an excess of non-silent mutations was determined using the methods previously described²⁵ and is described in detail in the supplemental methods Gene expression profiling. RNA was harvested from fresh frozen patient tissue with Trizol according to manufacturer's instructions (Invitrogen) and analyzed using human U133 Plus 2.0 Array probe sets according to manufacturer's instructions (Affymetrix). Summarized expression values were computed using the robust multichip average (RMA) approach, corrected for batch effects, and used for clustering analysis and discriminate gene analysis using a moderated t-statistic. The patient and cell line expression data were deposited with Gene Expression Omnibus and Array Express under accession numbers GSE17895 and E-TABM-770, respectively. Further detail on analysis can be found in the Supplemental Methods.

Supplementary Material

Refer to Web version on PubMed Central for supplementary material.

Acknowledgments

We would like to acknowledge the Wellcome Trust for support under grant reference 077012/Z/05/Z and the Hauenstein and Gerber Foundations for support for the microarray expression work. We also thank Sancha Martin, Wendy McLaughlin and Sabrina Noyes for administrative support and Francis Brasseur for providing the matched-pair ccRCC cell lines.

References

1. Eble, J.; Epstein, J.; Sesterhann, I. Pathology and Genetics of Tumours of the Urinary System and Male Genital Organs. IARC Press; Lyon, France: 2004.
2. Rini BI, Campbell SC, Escudier B. Renal cell carcinoma. *The Lancet*. 2009; 373:1119–1132.
3. van Haaften G, et al. Somatic mutations of the histone H3K27 demethylase gene UTX in human cancer. *Nat Genet*. 2009; 41:521–3. [PubMed: 19330029]
4. Banks RE, et al. Genetic and Epigenetic Analysis of von Hippel-Lindau (VHL) Gene Alterations and Relationship with Clinical Variables in Sporadic Renal Cancer. *Cancer Res*. 2006; 66:2000–2011. [PubMed: 16488999]
5. Bommi-Reddy A, et al. Kinase requirements in human cells: III. Altered kinase requirements in VHL-deficient cancer cells detected in a pilot synthetic lethal screen. *Proc Natl Acad Sci U S A*. 2008; 105:16484–16489. [PubMed: 18948595]
6. Chi JT, et al. Gene Expression Programs in Response to Hypoxia: Cell Type Specificity and Prognostic Significance in Human Cancers. *PLoS Med*. 2006; 3:e47. [PubMed: 16417408]
7. Jones S, et al. Core signaling pathways in human pancreatic cancers revealed by global genomic analyses. *Science*. 2008; 321:1801–6. [PubMed: 18772397]
8. Parsons DW, et al. An integrated genomic analysis of human glioblastoma multiforme. *Science*. 2008; 321:1807–12. [PubMed: 18772396]
9. Greenman C, et al. Patterns of somatic mutation in human cancer genomes. *Nature*. 2007; 446:153–158. [PubMed: 17344846]
10. Sun X-J, et al. Identification and Characterization of a Novel Human Histone H3 Lysine 36-specific Methyltransferase. *J. Biol. Chem*. 2005; 280:35261–35271. [PubMed: 16118227]
11. Iwase S, et al. The X-Linked Mental Retardation Gene SMCX/JARID1C Defines a Family of Histone H3 Lysine 4 Demethylases. *Cell*. 2007; 128:1077–1088. [PubMed: 17320160]
12. Issaeva I, et al. Knockdown of ALR (MLL2) Reveals ALR Target Genes and Leads to Alterations in Cell Adhesion and Growth. *Mol. Cell. Biol*. 2007; 27:1889–1903. [PubMed: 17178841]
13. Lee MG, et al. Demethylation of H3K27 Regulates Polycomb Recruitment and H2A Ubiquitination. *Science*. 2007; 318:447–450. [PubMed: 17761849]
14. Ferner RE. Neurofibromatosis 1 and neurofibromatosis 2: a twenty first century perspective. *Lancet Neurol*. 2007; 6:340–351. [PubMed: 17362838]
15. Gordan JD, Bertout JA, Hu C-J, Diehl JA, Simon MC. HIF-2 α Promotes Hypoxic Cell Proliferation by Enhancing c-Myc Transcriptional Activity. *Cancer Cell*. 2007; 11:335–347. [PubMed: 17418410]
16. Zhang H, et al. HIF-1 Inhibits Mitochondrial Biogenesis and Cellular Respiration in VHL-Deficient Renal Cell Carcinoma by Repression of C-MYC Activity. *Cancer Cell*. 2007; 11:407–420. [PubMed: 17482131]
17. Mandriota SJ, et al. HIF activation identifies early lesions in VHL kidneys: Evidence for site-specific tumor suppressor function in the nephron. *Cancer Cell*. 2002; 1:459–468. [PubMed: 12124175]
18. McKinnon PJ, Caldecott KW. DNA Strand Break Repair and Human Genetic Disease. *Annu Rev Genomics Hum Genet*. 2007; 8:37–55. [PubMed: 17887919]
19. Kudlow BA, Kennedy BK, Monnat RJ. Werner and Hutchinson-Gilford progeria syndromes: mechanistic basis of human progeroid diseases. *Nat Rev Mol Cell Biol*. 2007; 8:394–404. [PubMed: 17450177]

20. Demuth I, Digweed M. The clinical manifestation of a defective response to DNA double-strand breaks as exemplified by Nijmegen breakage syndrome. *Oncogene*. 2007; 26:7792–7798. [PubMed: 18066092]
21. DeMasi J, Huh K-W, Nakatani Y, MÃ¼nger K, Howley PM. Bovine papillomavirus E7 transformation function correlates with cellular p60 protein binding. *Proc Natl Acad Sci U S A*. 2005; 102:11486–11491. [PubMed: 16081543]
22. Huh K-W, et al. Association of the human papillomavirus type 16 E7 oncoprotein with the 600-kDa retinoblastoma protein-associated factor, p600. *Proc Natl Acad Sci U S A*. 2005; 102:11492–11497. [PubMed: 16061792]
23. Young AP, et al. VHL loss actuates a HIF-independent senescence programme mediated by Rb and p400. *Nat Cell Biol*. 2008; 10:361–369. [PubMed: 18297059]
24. Dicks E, et al. AutoCSA, an algorithm for high throughput DNA sequence variant detection in cancer genomes. *Bioinformatics*. 2007; 23:1689–1691. [PubMed: 17485433]
25. Greenman C, Wooster R, Futreal PA, Stratton MR, Easton DF. Statistical analysis of pathogenicity of somatic mutations in cancer. *Genetics*. 2006; 173:2187–98. [PubMed: 16783027]

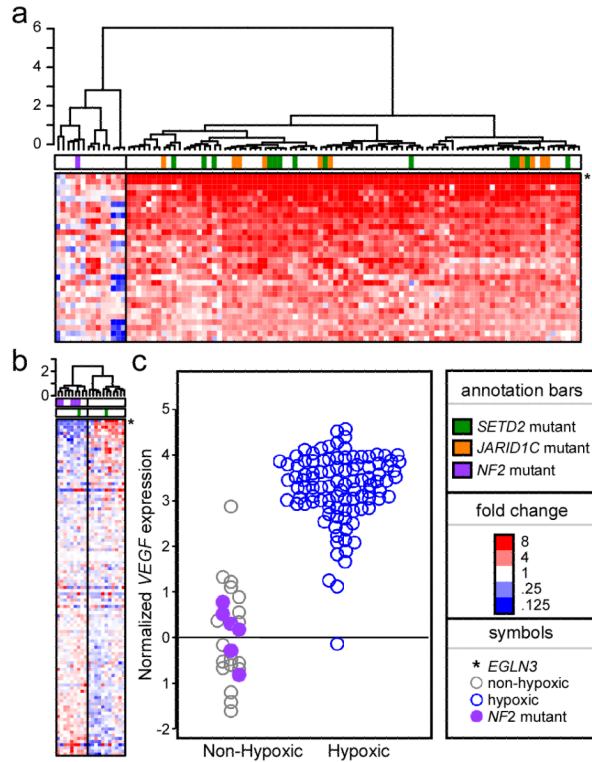


Figure 1. Gene expression analysis reveals two main classes of tumours - hypoxic and non-hypoxic

A. Heatmap of hypoxia related gene expression (see methods for source of gene list) in primary ccRCC tumours. Red colour indicates a relative increase in gene expression while blue indicates decreased expression. Samples clustered to the left (highlighted with grey bar) do not show a hypoxic gene expression pattern while those to the right display the hypoxic expression pattern. *EGLN3* is the most upregulated gene in the hypoxic group. *JARID1C* (orange bar) and *SETD2* (green bar) mutant tumours are all clustered in the hypoxic group while the *NF2* mutant tumour (purple bar) is in the non-hypoxic group. B. A similar pattern is observed in RCC cell lines with *EGLN3* again being the most upregulated gene in the hypoxic group. Five *NF2* mutant cell lines cluster in the non-hypoxic group. C. Clustering of *NF2* mutant samples within low VEGF expression/non-hypoxic subgroup of ccRCC.

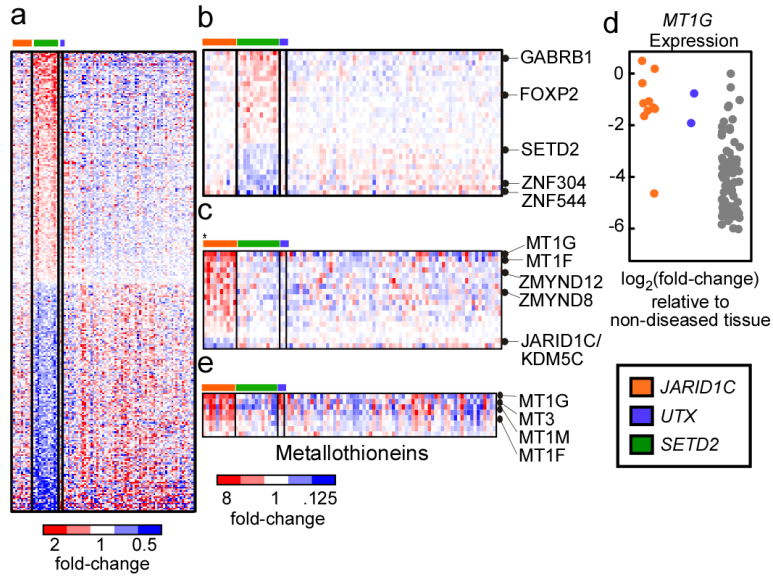


Figure 2. Gene deregulation in SETD2 and JARID1C/KDM5C mutant samples

A. Genes ($n=298$) that are deregulated in tumor samples that contain non-synonymous SETD2 mutations ($n=13$) versus samples that lack such mutations ($n=77$) are plotted as a heatmap. Red color indicates increased gene expression compared to the average expression in the tumor samples, blue color indicates decreased gene expression. B. The most significantly deregulated genes in the SETD2 mutant samples. C. Heatmap of genes ($n=18$) that are deregulated in tumor samples that contain non-synonymous JARID1C/KDM5C mutations ($n=10$) versus samples that lack such mutations ($n=80$). The asterisks (*) highlights the sample containing the S1222P mutation. D. Expression of the MT1G gene in the tumor samples. Expression values are shown relative to non-diseased tissue and \log_2 -transformed such that a \log_2 -transformed value of -2 is equivalent to a 4-fold decrease in expression relative to non-diseased kidney. E. Metallothionein genes ($n=8$) were isolated examined for deregulated expression in JARID1C and UTX mutant samples. Significantly deregulated genes are indicated.

Table 1

Patient demographics and clinical characteristics of primary ccRCC screening set

Sex	
Male	56
Female	40
Age, Years	
Median	62
Range	32–85
Stage at diagnosis	
I	44
II	14
III	34
IV	2
NA	2
Grade at diagnosis	
1	4
2	35
3	39
4	16
NA	2

Table 2

Mutation summary of highlighted genes in ccRCC

Gene	Initial Screen Mutations	Follow-up Screen Mutations	Additional RCC cell line mutations*	Total mutations
<i>HIF1A</i>	1 nonsense	1 splice/del, 1 frameshift		3
<i>JARID1C</i>	1 nonsense, 1 missense	5 nonsense, 2 splice/del, 4 frameshift, 1 missense		14
<i>MLL2</i>	1 nonsense, 2 missense	9 missense, 1 nonsense, 4 silent	ND	17
<i>NBN</i>	1 frameshift	1 frameshift	ND	2
<i>NF2</i>	3 frameshift, 1 splice	1 frameshift	1 nonsense, 1 splice/del	7
<i>PMS1</i>	1 frameshift	2 nonsense (Germline)		3
<i>SETD2</i>	4 frameshift, 1 nonsense, 2 missense	4 frameshift, 3 nonsense, 1 missense	1 frameshift	16
<i>UTX</i>	3 frameshift, 1 splice, 2 missense	1 frameshift, 1 splice/del, 3 missense, 1 nonsense (Germline)		12
<i>WRN</i>	1 nonsense	1 splice/frameshift, 1 missense	ND	3
<i>ZUBR1</i>	1 frameshift, 1 missense, 1 silent	3 frameshift, 4 missense	ND	10

* no matching normal sequence available, presumptive somatic mutation. ND=not done. Detailed mutation annotation can be found in Supplementary Table 8.